# The Influence of Fuel Injection Pressure on Economic Efficiency, Technical Parameters, and Emissions of 490QZL Diesel Engine

**Quynh Nguyen Thin**
Faculty of Mechanical Engineering, University of Transport and Communications, Hanoi, Vietnam
thinquynh@utc.edu.vn (corresponding author)

**Trung Tran Duc**
Faculty of Mechanical Engineering, University of Transport and Communications, Hanoi, Vietnam
bmdongluc@utc.edu.vn

*Received: 23 July 2025 | Revised: 11 September 2025 | Accepted: 27 September 2025*

 *DOI: https://doi.org/10.48084/etasr.13610*

## ABSTRACT

**The operation of a diesel engine is greatly affected by the fuel injection process. This process directly impacts fuel atomization and the spray's characteristic parameters, as well as the engine's economic efficiency, technical parameters, and emissions. The present study examines how increasing the fuel injection pressure affects the operating parameters of the 490 QZL diesel engine at maximum torque using a 3D model from the AVL Fire package. The results show that increasing the fuel injection pressure from 500 bar to 3,000 bar increases the power value by 19.7% and decreases the useful fuel consumption rate by 17.6%, with a fuel injection angle of 22 degrees before the Top Dead Center (TDC) remaining constant. Soot emission decreases by 44%, with a more significant decrease observed at injection pressures ranging from 1500 bar to 3000 bar. Nitrogen Oxide ($NO_x$) emissions slowly increase at injection pressures from 1000 bar to 1500 bar, but rapidly increase at injection pressures above 1500 bar. Hydrocarbon (HC) and Carbon Monoxide (CO) emissions decrease most markedly at injection pressures from 1000 bar to 2000 bar; at higher pressure values, the decrease is slower. Additionally, as the injection pressure increases, the length of the fuel spray increases significantly; however, the spray cone angle changes minimally due to the influence of the nozzle hole's geometrical size. Increasing the injection pressure improves the economic efficiency and technical parameters, while reducing the HC, CO, and especially soot emissions. These results form the basis for improving the diesel engine test bed at the Mechanical Laboratory of the University of Transport and Communications in Vietnam.**

***Keywords-diesel engine; 490QZL; fuel injection pressure; AVL Fire; emissions***

## I. INTRODUCTION

The European Union's assessment states that diesel engines will remain a primary power source for heavy trucks, road tractors, buses, construction machinery, and agricultural machinery. Similar predictions have been made for countries in Asia and Southeast Asia. The number of vehicles, especially those using diesel fuel, is increasing in Vietnam and around the world over time. Concurrently, the demand for engine power in L for vehicles that meet increasingly stringent environmental requirements has led to the need for further solutions to improve engine performance. Studied and applied solutions include redesigning engines to optimize the internal combustion engine details and systems [1], reducing the carbon content in fuels by using alternative and green fuels [2], as well as gas fuels and other energy sources from renewable resources [3] and using exhaust gas recirculation systems, Selective Catalytic Reduction (SCR) systems, and smoke filters [4, 5]. Theoretically, fuel injection pressure directly affects the fuel atomization and the spray's characteristic parameters, as well as the engine's technical and economic parameters. Therefore, increasing the injection pressure and the number of injections per cycle is a solution considered to improve atomization and air-fuel mixture mixing in the engine [6, 7]. Common rail fuel injection systems achieve an injection pressure of 1500 bar at an average pressure. High-pressure fuel injection systems can reach an injection pressure of 2000 bar and easily control the start and end points of the injection process. Furthermore, the system enables multi-stage injection control and provides an injection pressure that adapts to the operating modes of the actual working conditions. The injection volume, timing, and pressure are calculated and stored in the ECU and are independent of other conditions. Modern diesel engines use a new generation of fuel injection systems with an injection pressure that can reach 2,200 bar. Increasing the fuel injection pressure from 1500 bar to 2400 bar reduced the ignition delay

by nearly half and increased the engine efficiency. Additionally, the fuel combustion time in the combustion chamber decreased when this system was applied to a heavy-duty diesel engine [8]. It has been shown that increasing the fuel injection pressure in combination with decreasing the hole diameter gradually decreases the engine soot emissions. Micro-diameter nozzles combined with high injection pressure create a better mixture than conventional nozzles and increase the vaporization rate while reducing the homogenization time of the mixture in the combustion chamber [6]. High injection pressure, together with a small hole size, is highly efficient in increasing the turbulence velocity and reducing fuel particle size. The smoke level is lower at a constant $NO_x$ emission level when the injection pressure increases from 2000 bar to 2500 bar. Additionally, increasing the injection pressure significantly reduces the fuel consumption at a constant NOx and smoke emission level [9, 10]. The combustion process of a diesel engine depends greatly on the fuel injection process, including factors such as fuel injection pressure, fuel injection mass per cycle, fuel injection timing, and the number of injections per cycle. Studies were carried out with injection pressures reaching 2500 bar. The engine operating parameters were evaluated under test conditions and applied in practice. When increasing the injection pressure, issues such as sealing, injection process control, manufacturing materials, and component operating time must be considered and evaluated. Therefore, the impact of further increasing the pressure on the operating parameters of modern diesel engines needs to be considered, studied, and evaluated. Additionally, the effect of the injection pressure on the operating parameters of the engine differs greatly depending on the shape of the combustion chamber.

## II. THEORETICAL BASIS OF 3D MODEL IN AVL FIRE

### A. Fuel Injection Model

The spray model involves multiphase flow phenomena, thus necessitating the numerical solution of conservation equations for both gas and liquid phases. In the context of the liquid phase, the vast majority of spray calculations are predicated on a statistical method known as the discrete droplet method. The spray process is calculated using sub-models. The momentum exchanges between fuel droplets and air, turbulent dispersion, droplet evaporation, secondary breakup, droplet collisions, and droplet-wall interactions are performed by a comprehensive model suite that allows application to different flow regimes. The vapor of the fuel droplets is used as an input parameter to the supplementary equation for the vapor part. The solid particles can be calculated by the discrete droplet method. The trajectory and velocity of a particle or droplet are given by:

$$m_d \frac{du_{id}}{dt} = F_{idr} + F_{ig} + F_{ip} + F_{ivm} + F_{ib} \quad (1)$$

where $m_d$ is the particle mass, $u_{id}$ is the particle velocity vector, $F_{ip}$ is the force pressure, $F_{ivm}$ is the virtual mass force that takes into account the acceleration/deceleration of the surrounding the droplets, particles or bubbles, $F_{ib}$ other external forces, such as binding forces, magnetic or electrostatic forces, Magnus forces or other forces, $F_{idr}$ is the drag force, $D_p$ is a dual function, $F_{ig}$ is a force which includes the effects of gravity and buoyancy.

### B. Combustion Model

The study used the ECFM-3Z combustion model, where the average amounts of chemicals, such as $O_2$, $N_2$, $H_2$, and $H_2O$, were calculated based on transport equations. The term "burnt gases" refers to the actual combustion gases present in the mixed region $M^b$, a portion of the unmixed fuel in the region $F^b$, and air in the region $A^b$. The "burnt gases" can be defined as:

$$\frac{\partial \overline{\rho}\tilde{y}_X}{\partial t} + \frac{\partial \overline{\rho}\widetilde{u_i}\tilde{y}_X}{\partial x_i} - \frac{\partial}{\partial x_i}\left(\left(\frac{\mu}{S_C} + \frac{\mu_t}{S_{Ct}}\right)\frac{\partial \tilde{y}_X}{\partial x_i}\right) = \overline{\dot{\omega}}_X \quad (2)$$

where $\overline{\dot{\omega}}_X$ is the combustion source and $\tilde{y}_X$ is the average mass fraction of the i component, $S_C$ is the Schmidt number, and $S_{Ct}$ is the turbulent Schmidt number.

### C. Mixing Model

The K model is a method of calculating the mixture quantity with a characteristic time step. In order to develop a comprehensive model, it is important to ascertain the precise quantities of fuel that infiltrate both the mixture region and the "pure fuel" region during the process of evaporation. The pure fuel region is defined as region F, and the mixture region extends from region *F* to region *M*, as shown in Figure 1.

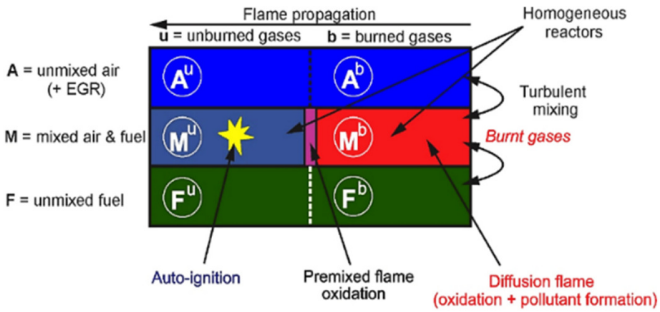


Fig. 1. Zones in the ECFM-3Z combustion model.

The fuel-air mixing process is simulated by initially placing the fuel in the "pure fuel" zone. This allows evaporated fuel from the droplet to be released into the fuel zone, resulting in: $F=F^u + F^b$. In order to describe the three mixing regions, two new quantities must be defined: unmixed fuel $\tilde{y}_{Fu}^F (\tilde{y}_{Fu}^F = \tilde{y}_{Fu}^{u,F} + \tilde{y}_{Fu}^{b,F})$ and unmixed oxygen $\tilde{y}_{O_2}^A (\tilde{y}_{O_2}^A = \tilde{y}_{O_2}^{u,A} + \tilde{y}_{O_2}^{b,A})$.

$$\frac{\partial \overline{\rho}\tilde{y}_{Fu}^u}{\partial t} + \frac{\partial \overline{\rho}\widetilde{u_i}\tilde{y}_{Fu}^u}{\partial x_i} - \frac{\partial}{\partial x_i}\left(\frac{\mu}{S_c}\frac{\partial \tilde{y}_{Fu}^F}{\partial x_i}\right) = \overline{\rho}\tilde{S}_{Fu}^F + \overline{\rho}\overline{\dot{E}}_{Fu}^{F\to M} \quad (3)$$

$$\frac{\partial \overline{\rho}\tilde{y}_{O_2}^A}{\partial t} + \frac{\partial \overline{\rho}\widetilde{u_i}\tilde{y}_{O_2}^A}{\partial x_i} - \frac{\partial}{\partial x_i}\left(\frac{\mu}{S_c}\frac{\partial \tilde{y}_{O_2}^A}{\partial x_i}\right) = \overline{\rho}\overline{\dot{E}}_{O_2}^{A\to M} \quad (4)$$

The mixing model is described by the sources $\bar{\dot{E}}_{Fu}^{F\to M}$ and $\bar{\dot{E}}_{O_2}^{A\to M}$ in the unmixed fuel and unmixed oxygen. The mixing quantity is calculated with a characteristic time scale based on the k-ε model:

$$\overline{\dot{E}}_{Fu}^{F\to M} = -\frac{1}{\tau_m}\tilde{y}_{Fu}^{F}\left(1-\tilde{y}_{Fu}^{F}\frac{\bar{\rho}M^{M}}{\rho^{-u}|uM_{Fu}}\right) \quad (5)$$

$$\overline{\dot{E}}_{O_2}^{A\to M} = -\frac{1}{\tau_m}\tilde{y}_{O_2}^{A}\left(1-\frac{\tilde{y}_{O_2}^{A}}{\tilde{y}_{O_2}^{\infty}}\frac{\bar{\rho}M^{M}}{\rho^{-u}|uM_{air+EGR}}\right) \quad (6)$$

where $M^M$ is the average molar mass of the mixed gases, $M_{Fu}$ is the mass of the fuel, $M_{O_2}$ is the mass of Oxygen, $M_{air+EGR}$ is the average mass of the unmixed gas + exhaust gas, $\bar{\rho}$ is the mean density, $\bar{\rho}^u|u$ is the density of the unburned gases (density of the new gases that would be obtained if combustion did not occurred), $\tilde{y}_{O_2}^{\infty}$ is the mass of oxygen, and $\tau_m$ is the mixing time. Furthermore, the 3D model in AVL Fire uses calculation models or sub-models, as depicted in Table I.

TABLE I. OTHER MODELS/SUB-MODELS IN AVL FIRE FOR THE 490QZL DIESEL ENGINE

| Modules | Model/sub-model |
|---|---|
| $NO_x$ | Extended Zeldovich |
| Soot | Kinetic Model |
| Wall interaction model | Walljet 1 |
| Breakup model | Wave |
| Evaporation model | Dukowicz |

### *D. 3D Meshing of the Combustion Chamber of the 490QZL Engine in AVL Fire*

The diesel engine simulation does not include the processes of intake and exhaust, which are omitted to reduce the calculation time, and the calculation begins with the closure of the Intake Valve (IVC). The mesh is formed in Figure 2, with the total number of cells being 86,856, the number of faces 1,283, the number of boundary faces 172, and the average cell size 1 mm. The parameters and mesh of the AVL fire are based on the shape of the 490 QZL engine piston bowl. The model of the combustion chamber, subsequent to meshing, is presented in Figure 2. The fundamental parameters of the 490 QZL diesel engine are illustrated in Table II.

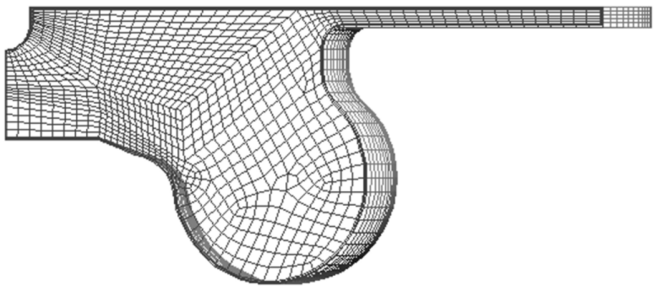

Fig. 2. 490 QZL engine combustion chamber model after meshing.

TABLE II. PARAMETERS OF THE 490 QZL DIESEL ENGINE

| Parameter | Value |
|---|---|
| Bore x stroke (mm) | 90x100 |
| Displacement volume, L | 2.54 |
| Compression ratio | 17 |
| Maximum power, kW | 52.5 |
| Speed to reach maximum power, RPM | 3200 |
| Maximum torque, N.m | 180 |
| Speed to reach maximum torque, RPM | 2000~2240 |
| Firing order | 1-3-4-2 |

## III. RESULTS AND DISCUSSION

The engine should be simulated with fuel injection pressure ranging from 500 bar to 3000 bar at 2200 rpm. This is the speed at which the engine reaches the maximum torque, making this mode a subject of interest for further examination. The fuel injection amount value was determined by measuring the value of the original engine before increasing the injection pressure. The value in question is measured at 48 mgr per cycle, and it is injected at -22 degrees below the crank angle (bTDC). The changes in the engine parameters are:

### *A. Variation of Pressure and Rate of Heat Release*

Figure 3 presents the variation of pressure and the Rate of Heat Release (RoHR) within the cylinder in relation to the crankshaft angle under varying fuel injection pressures. An increase in fuel injection pressure from 500 bar to 3000 bar accelerates and intensifies the combustion process, as evidenced by the elevated peak of the RoHR, which occurs at a more rapid and premature time. This results in a substantial increase in the average pressure within the cylinder, particularly in the near-TDC region (approximately 725° CA), where the primary combustion process occurs. Specifically, at elevated injection pressures (2000 bar and above), the RoHR exhibits a sudden increase, reaching a higher peak value. This, in turn, results in an earlier and higher average pressure peak within the cylinder compared to low pressure levels.

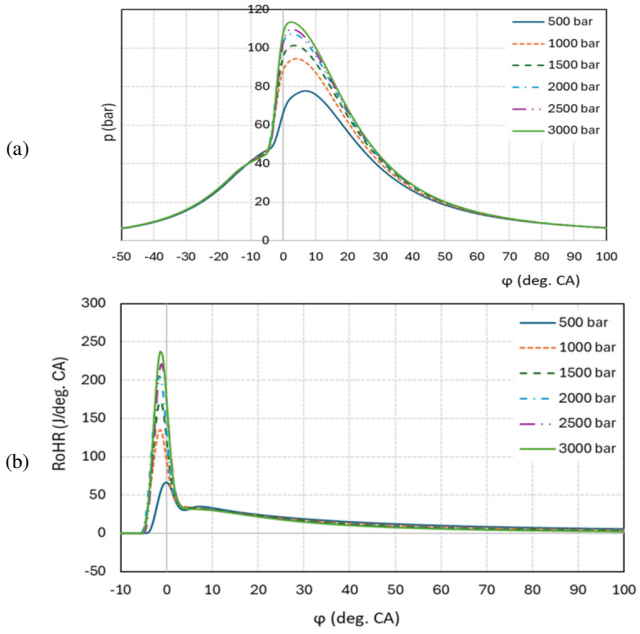


Fig. 3. Pressure and RoHR of the engine: a) pressure in the cylinder, b) RoHR.

Conversely, at low injection pressures (500 bar–1000 bar), the combustion process is slow and extended, resulting in a more gradual increase in pressure within the cylinder and a reduced pressure peak. This relationship directly reflects the effect of the combustion rate on the work process in the cylinder. When the combustion process occurs fast and is concentrated near the TDC, the pressure in the cylinder will

reach a greater value at the time the piston begins to move down, thereby contributing to increased work efficiency. However, an increase in pressure and heat dissipation rate concomitantly augments the thermal and mechanical load on the engine components. This phenomenon is accompanied by the risk of elevated NOx emissions, contingent upon inadequate adjustment.

### *B. Temperature Variation in the Combustion Chamber*

Figure 4 demonstrates that the temperature variation in the combustion chamber of a diesel engine depends on the crank shaft angle and the injection pressure level.

An analysis of the results reveals that, at the time near the TDC (approximately 725 degrees CA), the temperature inside the combustion chamber increases sharply in all injection modes. This is due to the rapid combustion reaction, which generates a significant amount of heat. As the piston moves downwards, it gradually decreases in temperature in accordance with the expansion process. The increases in injection pressure result in elevated maximum temperatures, ranging from approximately 1700 K to over 2200 K. This phenomenon indicates that elevated injection pressure leads to the atomization of fuel particles into smaller sizes, accelerating the evaporation process and enhancing the mixing with air. The result of this process is an accelerated and more efficient combustion reaction. Furthermore, the temperature at elevated injection pressure levels exhibits a rapid decline post-peak, indicative of the efficacy of the mixture and combustion process within the engine.

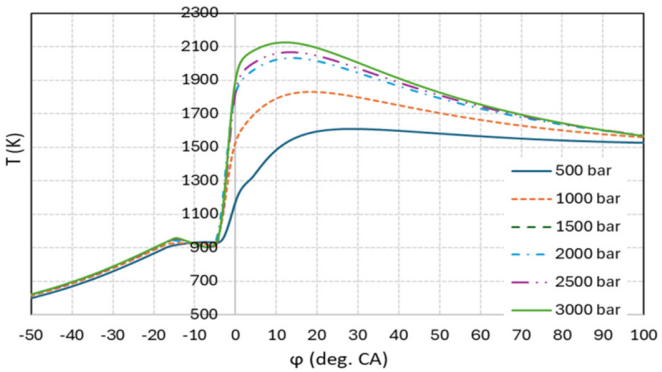


Fig. 4. Temperature variation in the combustion chamber according to fuel injection pressure.

### *C. Variation of Economic Efficiency and Technical Parameters of the Engine*

The present study examines the impact of the injection pressures on the economic efficiency and technical parameters of the engine. The investigation considers a range of parameters, including average effective pressure ($p_e$), brake torque ($M_e$), brake power ($N_e$), brake specific fuel consumption ($g_e$), and brake efficiency ($\eta_e$). An increase in injection pressure results in the fuel being injected at a higher speed, the fuel particles being smaller, and a significantly improved ability to mix with air in the combustion chamber. This facilitates the acceleration of the combustion process, resulting in fast combustion near the TDC. Consequently, the maximum combustion pressure in the cylinder is increased, thereby improving the engine's power generation capability. Figure 5 shows the simulation results of $M_e$, $N_e$, and $g_e$ as the fuel injection pressure is modified. It was observed that the power $N_e$ increased in proportion to the increase in injection pressure $p_{inj}$. The increase in $N_e$ is the most significant at injection pressures ranging from 500 bar to 1500 bar. Conversely, at higher pressure levels, the rate of increase exhibits a substantial decline, resulting in a more uniform curve. Concurrently, the $M_e$ also increases in accordance with the $N_e$ as the fuel injection pressure rises. Conversely, as the $p_{inj}$ increases, the $g_e$ decreases, when the fuel injection pressure ranges from 500 bar to 1500 bar. However, the rate of decrease exhibits a substantial decline at elevated pressures. The decline in the $g_e$ as the $p_{inj}$ rises signifies that the engine is operating in a more efficient manner, using fuel more productively. The enhanced combustion process is characterized by its increased efficiency and rapidity, leading to the conversion of a greater proportion of the fuel's chemical energy into useful mechanical work. This improvement leads to a reduction in energy loss due to under-combustion, thereby optimizing the overall efficiency of the combustion process.

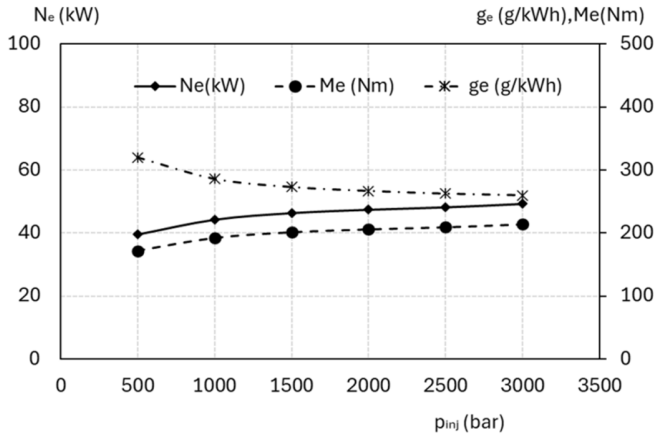


Fig. 5. Changes in brake power, brake torque, and brake specific fuel consumption, according to fuel injection pressure.

### *D. Variation of Brake Mean Effective Pressure and Brake Efficiency*

Figure 6 presents a notable variation trend of $p_e$ and brake efficiency $\eta_e$, with $p_{inj}$ ranging from 500 bar to 3000 bar. In general, both parameters tend to increase as the injection pressure increases. As the initial pressure $p_{inj}$ increases from approximately 500 bar to 3,000 bar, the peak pressure $p_e$ rises from 7.3 bar to 9.1 bar, and the efficiency index $\eta_e$ increases from 26% to 33%. The reduction in fuel droplet size, caused by the high injection pressure, results in enhanced air-fuel miscibility and an improved combustion process. At low injection pressures, the droplet size is increased, resulting in reduced mixing and an extended ignition delay, decreasing the efficiency. It appears that if the pressure is increased excessively, the ignition delay becomes significantly brief, the mixture does not have adequate time to homogenize, and the injection spray is excessive, it may come into contact with the

cylinder wall, leading to the formation of a fuel film that is challenging to burn completely. Consequently, there is a decline in the overall efficiency of the engine.

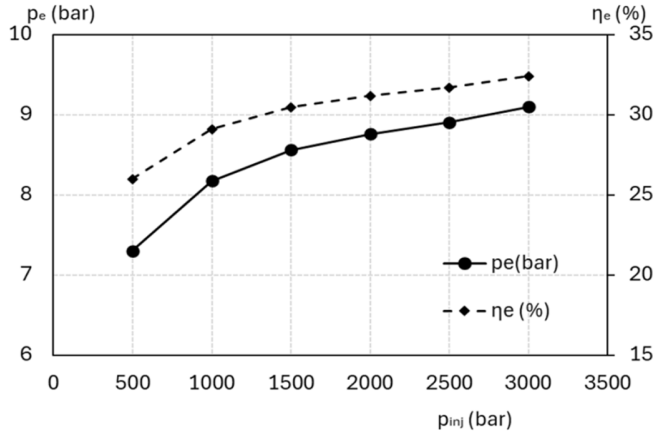


Fig. 6. Variation of brake mean effective pressure and brake efficiency with changing fuel injection pressure.

### *E. Engine Emission Variation*

As the injection pressure increases, $NO_x$ emissions exhibit a substantial rise, as shown in Figure 7. The increase in $NO_x$ emissions is characterized by a gradual rise at low injection pressures (below 1000 bar -1500 bar) and a subsequent rapid acceleration at higher pressure levels. At a pressure of 500 bar, the $NO_x$ value approaches zero. As the injection pressure increases, the $NO_x$ value exhibits a gradual increase, reaching 0.23 g/kWh at 1500 bar. The $NO_x$ value exhibited an accelerated increase as the injection pressure continued to rise, reaching its maximum at the highest injection pressure that was examined. The formation of $NO_x$ is found to be strongly dependent on two factors: the peak combustion temperature and the presence of oxygen. Elevated injection pressure results in the atomization of fuel particles into a finer dispersion, accelerated mixing processes, intensified combustion, and an approach to the TDC. Consequently, the peak temperature in the combustion chamber is elevated, significantly enhancing the chemical reactions that generate $NO_x$ from the nitrogen and oxygen present in the intake air.

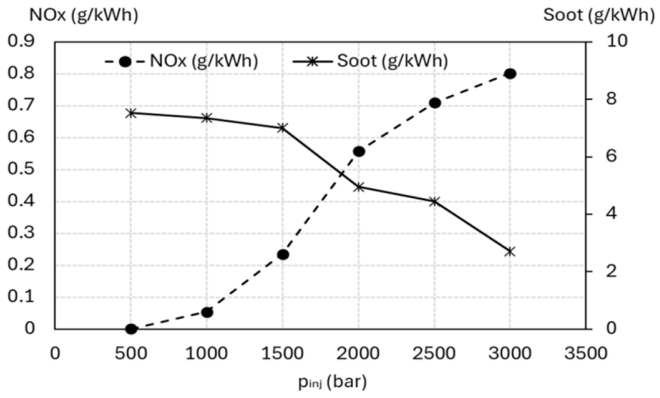


Fig. 7. Variation of $NO_x$ and soot emissions as fuel injection pressure changes.

The formation of soot is observed in regions characterized by oxygen deficiency and elevated temperatures within the combustion chamber. These conditions, namely the presence of fuel-rich environments and relatively high temperatures, are conducive to the formation of soot. The application of high injection pressure results in the formation of smaller fuel particles, thereby increasing the contact surface area and the fuel's capacity to penetrate the air. This results in the rapid and uniform mixing of fuel and air, thereby reducing the formation of regions with excessive fuel concentrations. Consequently, the combustion process is more complete, leading to a reduction in the amount of soot formed and an enhancement in the oxidation of the formed soot. The level of soot emissions is reduced more significantly in the range of 1500÷3000 bar. The CO and HC emissions are two critical indicators that reflect the extent of the combustion process completion in diesel engines. The simulation results demonstrate that the injection pressure exerts a discernible influence on the combustion process, consequently affecting the direct emissions of CO and HC. Figure 8 demonstrates that:

- In the range of 500 bar to 1000 bar, there is a significant increase in the effectiveness of the substance. The CO value exhibited a precipitous decline, dropping from 135.7 to 55.0 g/kWh (–60%), while the HC value experienced a more modest reduction, dropping from 0.0205 to 0.0131 g/kWh (–36%). It is evident that increasing the injection pressure in the initial stage results in a substantial reduction in fuel droplet size, a notable improvement in evaporation surface area, and a significant enhancement in the mixing with air. Consequently, the oxygen-deficient zone is considerably reduced, leading to a substantial decrease in CO and HC emissions.
- In the range of 1000 bar-2500 bar, there is a significant increase in the rate of change. The CO concentration exhibited a decline from 55.0 g/kWh to 3.8 g/kWh, while the HC concentration decreased from 0.01 g/kWh to 0.0075 g/kWh. At this stage, the injection pressure has caused the atomization of the spray to reach relatively good levels. As a result, the impact of increasing pressure is primarily observed in small dead zones and cylinder gaps. Increased injection pressure was found to result in increased spray length, with the combustion center area gradually moving closer to the cylinder wall. The atomization capability and the extent of air usage in the space areas distant from the nozzle result in a reduction of CO and HC.
- In the range of 2500 bar to 3000 bar, the emission reduction effect slows down, as the atomization level is saturated and the air level in the combustion chamber is depleted. Consequently, the levels of CO and HC exhibit fluctuations with minimal variations. It was observed that the injection pressure, ranging from 1000÷2000 bar, resulted in a substantial reduction in the CO and HC emissions. As a result, the phenomenon of saturation and the side effects are prevented, as the mechanism of reducing the droplet size and enhancing mixing occurs prior to the occurrence of these effects at higher pressure levels.

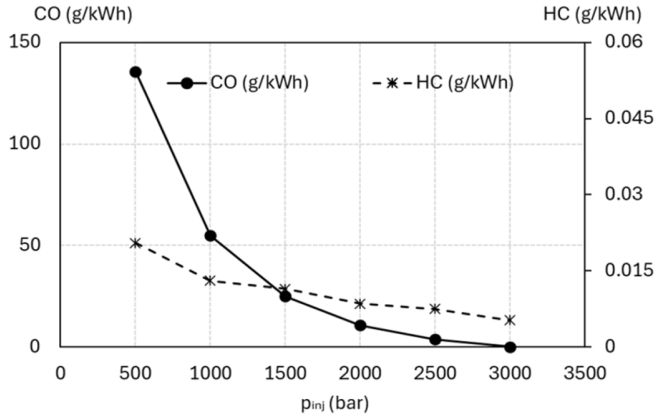


Fig. 8. Variation of CO and HC emissions according to fuel injection pressure.

### *F. Effect of Injection Pressure on Fuel Spray Development*

Figure 9 presents the variation in the spray cone angle and fuel spray length, in relation to the fuel injection pressure. It appears that when the fuel injection pressure is increased from 500 bar to 3000 bar, there is a significant increase in the length of the fuel spray. Increasing the injection pressure increases the energy provided to the fuel spray, resulting in a longer spray under constant pressure conditions in the combustion chamber. With regard to the spray cone angle, its modification in response to the injection pressure is minimal, attributable to the impact of the geometric dimensions of the fuel injection opening. The development of the fuel spray is observed through the 3D simulation software, as shown in Table III. The spray tips are in motion and rapidly approaching the walls of the combustion chamber. As the fuel injection pressure increases, a greater quantity of fuel will vaporize and burn. The fuel droplets will undergo a more rapid heating process, resulting in a greater proportion of energy expenditure during the fuel spray's movement. As a consequence, a reduced quantity of fuel falls on the cylinder wall, thereby increasing the amount of heat generated due to the increased amount of fuel injected into the combustion chamber.

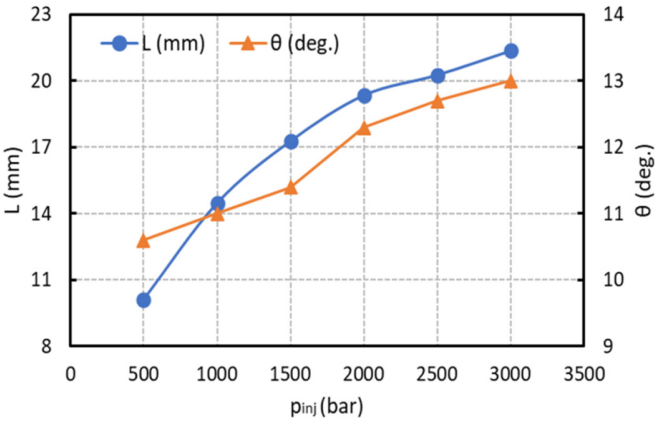


Fig. 9. Variation of the spray cone angle and fuel spray length with injection pressure at -20 deg. CA bTDC.

TABLE III. FUEL SPRAY DEVELOPMENT AND TEMPERATURE FIELD IN THE COMBUSTION CHAMBER ACCORDING TO FUEL INJECTION PRESSURE AT -20 DEG. CA BTDC

| $p_{inj}$ | $L$ (mm) | $\theta$ (deg.) |
|---|---|---|
| 500 | 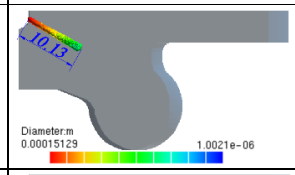  | 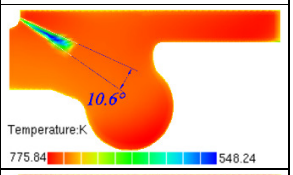  |
| 1000 | 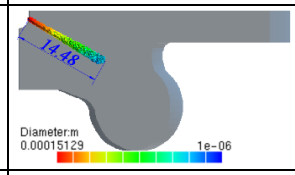  | 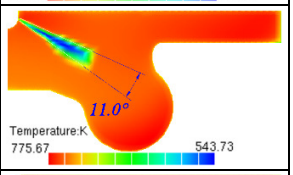  |
| 1500 | 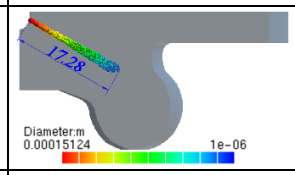  | 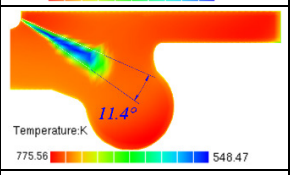  |
| 2000 | 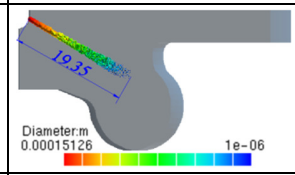  | 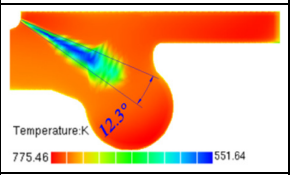  |
| 2500 | 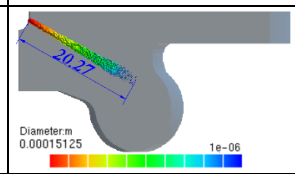  | 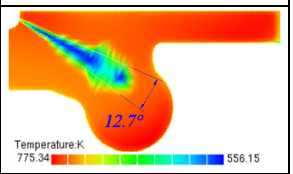  |
| 3000 | 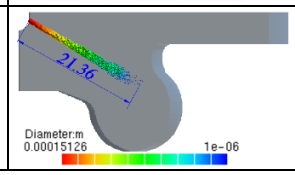  | 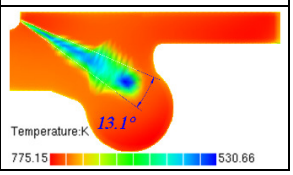  |

In general, when fuel is injected into the combustion chamber for a longer time, it receives more heat because the total surface area of the fuel droplets that contact the hot compressed air in the cylinder increases. The phenomenon of heat transfer from gas to fuel is highly dependent on several variables, including injection pressure, pressure, and temperature in the combustion chamber. The fuel that falls on the cylinder wall will vaporize and evaporate quickly, but the combustion time will still be quite long. As the pressure increases further, it becomes evident that the fuel undergoes an increase in temperature and more concentrated combustion near the TDC. The injection pressure increase must be adjusted accordingly to the structure of the combustion chamber and the angle of the injection hole to limit fuel sticking to the wall, which negatively affects the combustion process of the diesel engine.

## IV. CONCLUSIONS

The present study examined the impact of increasing fuel injection pressure on the economic efficiency, technical parameters, and emissions of a diesel engine, using a three-dimensional simulation model. The outcomes of this study are:

- The increases in fuel injection pressure result in improvements in the brake power, brake torque, brake mean effective pressure, and brake efficiency of the engine. Concurrently, there is a gradual decrease in the fuel consumption of the engine. The brake power value exhibited an increase of 19.7% at a constant fuel injection angle. The injection pressure demonstrated an escalation from 500 bar to 3000 bar, while the brake-specific fuel consumption decreased by 17.6%.
- The emissions of soot, Carbon Monoxide (CO), and Hydrocarbon (HC), exhibited a gradual decrease, whereas the Nitrogen Oxide ($NO_x$) emissions increased in response to an increase in fuel injection pressure. The soot value demonstrated a decrease of up to 44%, exhibiting a steady decline with increasing injection pressure. The reduction in soot value seemed to become more evident at pressures ranging from 1500 bar to 3000 bar. Conversely, the $NO_x$ increase is characterized by a gradual rise at low injection pressure and a rapid acceleration at higher pressures. The integration of Selective Catalytic Reduction (SCR) on the exhaust pipe enhances the efficacy of NOx treatment while reducing soot emissions, thereby minimizing the risk of particulate filter blockage. For HC and CO, the injection pressure within the range of 1000 bar to 2000 bar results in the most evident emission reduction effect. The basis for this phenomenon can be attributed to the mechanism of reducing the droplet size and enhancing mixing, which occurs prior to the occurrence of saturation and side effects at higher injection pressure.
- Increasing the injection pressure provides greater energy to the spray, resulting in a longer spray under constant pressure conditions within the combustion chamber. Consequently, when the fuel injection pressure is increased from 500 bar to 3000 bar, the length of the fuel spray experiences a substantial increase. With regard to the spray cone angle, its modification in response to the injection pressure is minimal, attributable to the impact of the geometrical dimensions of the fuel injection orifice.

## REFERENCES

[1] Y. Liu, J. Lei, X. Deng, Y. Liu, D. Sun, and Y. Zhang, "Research and analysis of a thermal optimisation design method for aluminium alloy pistons in diesel engines," *Case Studies in Thermal Engineering*, vol. 52, Dec. 2023, Art. no. 103667, https://doi.org/10.1016/j.csite.2023.103667.

[2] S. Bhangwar *et al.*, "Analysis of Particulate Matter Emissions and Performance of the Compression Ignition Engine Using Biodiesel Blended Fuel," *Engineering, Technology & Applied Science Research*, vol. 12, no. 5, pp. 9400–9403, Oct. 2022, https://doi.org/10.48084/etasr.5204.

[3] K. Uddeen, Q. Tang, H. Shi, and J. Turner, "Performance and emission analysis of ammonia-ethanol and ammonia-methane dual-fuel combustion in a spark-ignition engine: An optical study," *Fuel*, vol. 358, Feb. 2024, Art. no. 130296, https://doi.org/10.1016/j.fuel.2023.130296.

[4] G. Boccardo *et al.*, "Experimental investigation on a 3000 bar fuel injection system for a SCR-free non-road diesel engine," *Fuel*, vol. 243, pp. 342–351, May 2019, https://doi.org/10.1016/j.fuel.2019.01.122.

[5] J. M. López, F. Jiménez, F. Aparicio, and N. Flores, "On-road emissions from urban buses with SCR + Urea and EGR + DPF systems using diesel and biodiesel," *Transportation Research Part D: Transport and Environment*, vol. 14, no. 1, pp. 1–5, Jan. 2009, https://doi.org/10.1016/j.trd.2008.07.004.

[6] Thìn Q. N., Hoai D. L., and Cao V. N., "Experimentally determine the effect of pressure on injection mass and development of the diesel fuel spray," *Transport and Communications Science Journal*, vol. 75, no. 6, pp. 1934–1947, 2024, https://doi.org/10.47869/tcsj.75.6.1.

[7] A. Vidal Roncero, P. Koukouvinis, and M. Gavaises, "Effect of Diesel injection pressures up to 450MPa on in-nozzle flow using realistic multicomponent surrogates," presented at the ILASS 2019 - 29th European Conference on Liquid Atomization and Spray Systems, Paris, France, Aug. 2019.

[8] M. Imperato, O. Kaario, T. Sarjovaara, and M. Larmi, "Influence of the in-cylinder gas density and fuel injection pressure on the combustion characteristics in a large-bore diesel engine," *International Journal of Engine Research*, vol. 17, no. 5, pp. 525–533, June 2016, https://doi.org/10.1177/1468087415589043.

[9] Q. Xu *et al.*, "Diesel Spray Characterization at Ultra-High Injection Pressure of DENSO 250 MPa Common Rail Fuel Injection System," presented at the SAE World Congress Experience, Detroit, MI, USA, Mar. 2017, pp. 2017-01–0821, https://doi.org/10.4271/2017-01-0821.

[10] W. Vera-Tudela, R. Haefeli, C. Barro, B. Schneider, and K. Boulouchos, "An experimental study of a very high-pressure diesel injector (up to 5000 bar) by means of optical diagnostics," *Fuel*, vol. 275, Sept. 2020, Art. no. 117933, https://doi.org/10.1016/j.fuel.2020.117933.